ISSN 1687- 0530

JES

JOURNAL OF ENGINEERING SCIENCES

Vol. 31-No.2 April 2003

Published By

FACULTY OF ENGINEERING- - UNIVERSITY OF ASSIUT -EGYPT

Journal of Engineering Sciences, Assiut University, Vol. 31, No. 2, pp. 305-320, April 2003

HEAT AND MASS TRANSFER BETWEEN AIR AND DESICCANT FALLING FILM IN A FINNED-TUBE ARRANGEMENT FOR DIFFERENT FLOW CONFIGURATIONS

S.A. Nada
Assistant Professor, Benha Higher Institute of Technology, Mechanical Engineering Department, Benha 13521, Egypt

(Received October 28, 2002 Accepted February 27, 2003)

The heat and mass transfer between a falling liquid film of calcium chloride desiccant solution and air in a rectangular finned-tube arrangement was studied numerically. The study was carried out for three different flow configurations: parallel, counter and cross flow of air with respect to the falling liquid film of the desiccant solution. For each flow configuration, the governing equations which relate air temperature, air humidity, liquid desiccant temperature, liquid desiccant concentration and plate surface temperature distribution were derived together with the appropriate boundary conditions. A finite difference technique was developed to solve these equations. The performance of the fin-tube arrangement for air dehumidification and liquid desiccant regeneration at various operating conditions for the three different flow configurations was studied. The effects of the inlet conditions of the air and desiccant film, their mass flow rates and the fin temperature on the air dehumidification process or the liquid desiccant regeneration process were predicted. Correlations were developed to predict the rate of heat and mass transfer between the air and the desiccant film for the three air flow configurations.

KEYWORDS: *Heat and mass transfer, liquid desiccant, finned-tube*

1. INTRODUCTION

Two different methods can be used for air dehumidification in air-conditioning applications which require low moisture and temperature control level. The first method is chilling the air below its dew point temperature using a vapour compression cooling system. The second method is to use desiccant system. If air is chilled to subfreezing dew point, the desiccant system must be used, with the desiccant may be solid or liquid.

Packed beds have been successfully used in the last twenty years for air dehumidification using liquid desiccant. Several researches were carried out to predict mathematically or experimentally the performance of packed beds under various

NOMENCLATURE

B	width of the fin, m
C_p	specific heat, J/kg.K
D_a	mass diffusivity of water vapour in air, m^2/s
D_d	mass diffusivity of water in desiccant, m^2/s
d_h	hydraulic diameter, m
f_s	fin spacing, m
g	acceleration of gravity , m/s^2
H	fin height, m
h_{fg}	latent heat of water , J/kg
h	local heat transfer coefficient at interface, $W/m^2.K$
$\overline{h}$	average heat transfer coefficient, $W/m^2.K$
$\overline{h}_m$	average mass transfer coefficient, $kg/m^2.s$
k	thermal conductivity, W/m.K
m_a	air mass flow rate, kg/s
m_d	desiccant mass flow rate per unit width of the fin, kg/s.m
$\overline{Nu}$	average Nusselt number at air side $(4\delta_a \overline{h} / k_a)$
P	pressure of air, Pa
Pr	Prandtl number $(\mu_a C_p / k_a)$
Re	Reynolds number $(4\delta_a \overline{u}_a / \nu_a)$
$\overline{Sh}$	average Sherwood number in air side $(4\delta_a \overline{h}_m / \rho_a D_a)$
Sc	Schmidt number $(\mu_a / \rho_a D_a)$
T	temperature, °C
$\overline{T}$	average temperature, °C
u	velocity in x direction, m/s
$\overline{u}_a$	average velocity of air, m/s
ω^*	equilibrium humidity ratio of air in contact with liquid desiccant, kg_w / kg_{da}
ω	humidity ratio, kg_w / kg_{da}
$\overline{\omega}$	average humidity ratio, kg_w / kg_{da}
x	coordinate in the direction of the film flow, m
y	coordinate perpendicular to the film flow, m
z	coordinate along the width of the film, m
α_d	thermal diffusivity of liquid desiccant, m^2/s
α_a	thermal diffusivity of air, m^2/s
δ_d	film thickness of liquid desiccant, m
δ_a	half of the thickness of air passage, m
ζ	mass concentration ratio of water in the liquid solution
η	coordinate in air flow direction, m
μ	dynamic viscosity, Pa.s
ρ	density, kg/m^3
ν	kinematic viscosity, m^2/s

Subscripts

a	air
av	average
b	base value
d	desiccant
i	inlet
int	interface
o	oulet
w	wall

design and operating conditions when using different types of liquid desiccant [1-4]. Packed beds, however, have two major disadvantages. The first one is the large pressure drop in the air side which leads to higher fan power. The second is the large ratio of desiccant mass flow rate to air flow rate.

To overcome these disadvantages, falling film of liquid desiccant was thought of as better than the packed bed configuration. Khan and Ball [5] carried out an experimental study to compare the predicted performance of a commercially available coil type liquid desiccant cooling and dehumidification system at part load conditions. Park et al. [6] studied numerically the heat and mass transfer between air in a cross flow and the falling film of desiccant flow over the fin surface of a heat exchanger. They used a finite difference method for the air and liquid flows in the exchanger. In their study the mathematical prediction of the outlet conditions of the air and liquid desiccant film from the plate-finned-tube heat exchanger encountered several difficulties. The reasons for these difficulties are that the governing equations are three dimensional, non-linear, coupled partial differential equations. Solving these equations is usually obtained by finite difference techniques through an iterative procedure. Rahmah et al. [7] studied numerically the heat and mass transfer process between falling liquid desiccant film and air in parallel flow heat exchanger. The effects of the inlet conditions of the air and the liquid desiccant film and their flow rates on the process were also predicted by the model.

In the present study, a model was developed to study parallel, counter and cross flow of air with respect to desiccant liquid falling film in a fin tube arrangement. To overcome the numerical difficulties in the study of Park et al. [6] for cross flow, the plate-finned-tube exchanger is considered to be consisting of several cells with each cell as shown in Fig. 1. The study was carried out for a single cell. The correlations developed to predict the heat and mass transfer coefficients between air and liquid desiccant film for this single cell can be used to predict the performance of the plate-fin-tube heat exchanger without the need to use finite difference grid to cover the whole exchanger. Therefore, the present study has two main objectives: (1) to show which flow configuration is superior to the others at various operating conditions, and (2) to develop correlations for the heat and mass transfer coefficients involved for the various processes of the arrangement under consideration.

2. MATHEMATICAL FORMULATION

2.1 Physical Model

Consider the fin-tube-arrangement shown in Fig. 1. In this arrangement a falling film of desiccant solution flows on the vertical surface of the fins while air flows in the gap between the fins. The air flow can be in the same direction of the film flow, i.e. parallel flow, or in the opposite direction with the film flow, i.e. counter flow, or in the perpendicular direction of the film flow, i.e. cross flow (see Fig. 2). Select a coordinate system as shown in Fig. 1: x coordinate in the direction of the film flow, y coordinate perpendicular to the film flow and z coordinate along the width of the fin. Define y_a and y_d coordinates in the air and desiccant film as shown in Fig. 3. The thickness of the desiccant film is designated by δ_d, the thickness of the air passage is designated by $2\delta_a$ and the fins spaces is designated by f_s, where $f_s = 2\delta_a + 2\delta_d$.

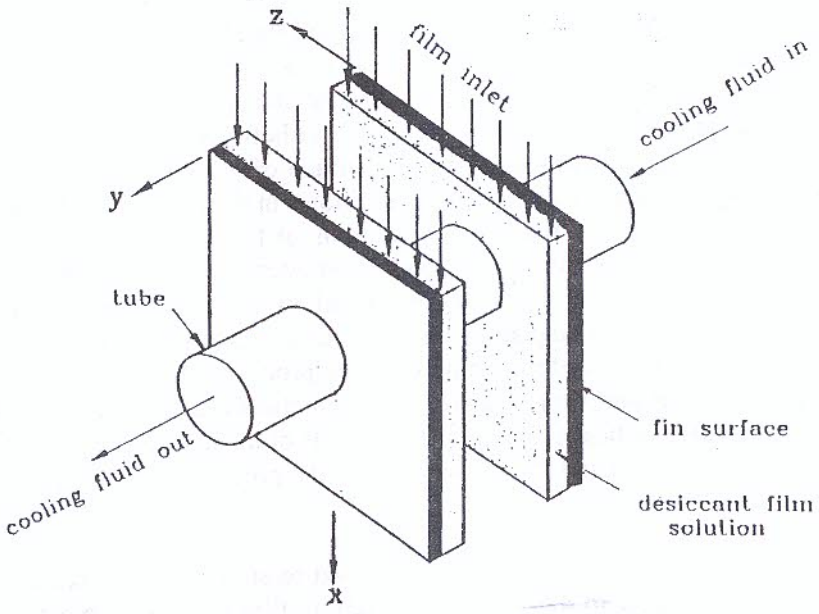

Fig. 1 Geometry of a cell of a plate-finned tube heat exchanger

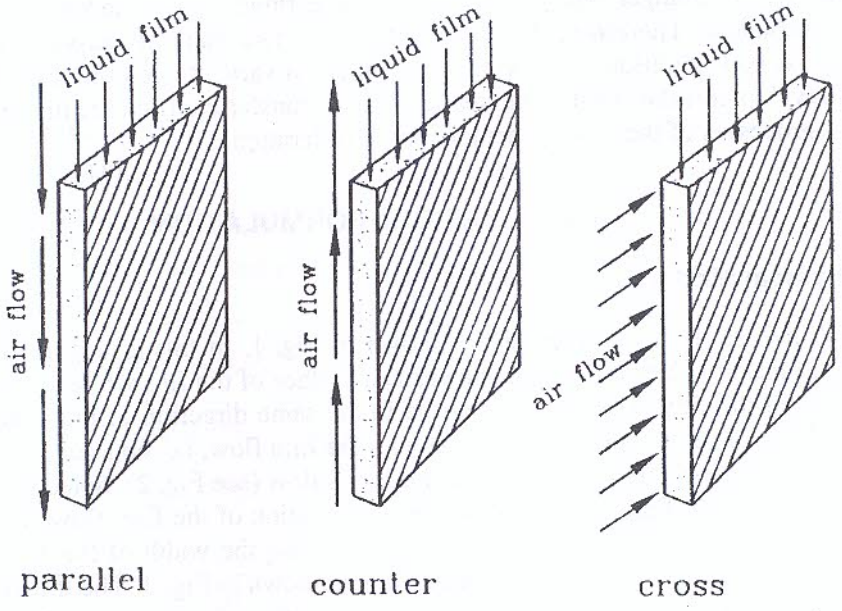

Fig. 2 Different flow configurations between air and desiccant film

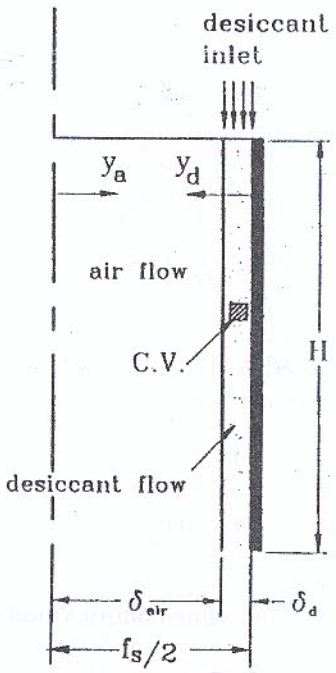

Fig. 3 The control volume of the liquid desiccant

The following assumptions are considered in deriving the governing equations:

1. Laminar, steady, and one dimensional flow.
2. Constant physical properties of both the liquid desiccant and air.
3. Thermodynamic equilibrium exists at the air-liquid desiccant interface.
4. Rate of water adsorption or desorption is negligible compared to the mass of the desiccant liquid flow.
5. The heat of adsorption is negligible compared to h_{fg}.
6. The thickness of the liquid desiccant film is constant along the height of the fin.
7. The drag of the air on the liquid film at the interface is negligible.
8. The velocity profiles of air and desiccant are fully developed at the entrance.
9. Body force of the air is negligible.
10. Heat conduction in both the x and z directions are negligible for the air and liquid.
11. The effect of the tube geometry on the heat and mass transfer processes between the air and the desiccant film is negligible.

The last assumption was validated experimentally by Park et al. [6]. Also, Rahmah et al. [7] showed by means of analysis for parallel flow that the relative error in the estimation of the rate of heat transfer between air and desiccant film is about 2 % when neglecting the tube geometry.

2.2 Basic Equations

Using the above assumptions, the energy and water concentration equations for a control volume in the desiccant film (see Fig. 3) can be written in the following form

$$u_d \frac{\partial T_d}{\partial x} = \alpha_d \frac{\partial^2 T_d}{\partial y_d^2} \tag{1}$$

$$u_d \frac{\partial \zeta}{\partial x} = D_d \frac{\partial^2 \zeta}{\partial y_d^2} \tag{2}$$

The above equations are subjected to the following boundary conditions at the air entrance and at the liquid-fin interface :

$$\text{at} \quad x = 0: \qquad T_d = T_{di}, \quad \zeta = \zeta_i \tag{3}$$

$$\text{at } y_d = 0: \qquad T_d = T_w, \quad \frac{\partial \zeta}{\partial y_d} = 0 \tag{4}$$

The x-momentum equation for the same control volume in the desiccant film gives

$$\upsilon_d \frac{\partial^2 u_d}{\partial y_d^2} + g = 0 \tag{5}$$

where υ_d is the desiccant kinematic viscosity and g is the gravitational acceleration. This equation is subjected to the boundary conditions: $u_d = 0 \; at \; y_d = 0$ and $\partial u_d / \partial y_d = 0 \; at \; y_d = \delta_d$ (No drag between the air and the liquid film at the interface). Solving Eq. (5) with its boundary conditions, the velocity distribution of the desiccant film is obtained as

$$u_d = \frac{g}{\upsilon}(\delta_d y_d - \frac{1}{2} y_d^2) \tag{6}$$

The continuity equation at any cross section of the desiccant flow gives the expression for the film thickness as

$$\delta_d = (3 \dot{m}_d \upsilon_d / B \rho_d g)^{1/3} \tag{7}$$

Similarly, the energy equation and moisture mass balance of a control volume in the air flow (see Fig. 4) give the following equations

$$u_a \frac{\partial T_a}{\partial \eta} = \alpha_a \frac{\partial^2 T_a}{\partial y_a^2} \tag{8}$$

$$u_a \frac{\partial \omega}{\partial \eta} = D_a \frac{\partial^2 \omega}{\partial y_a^2} \tag{9}$$

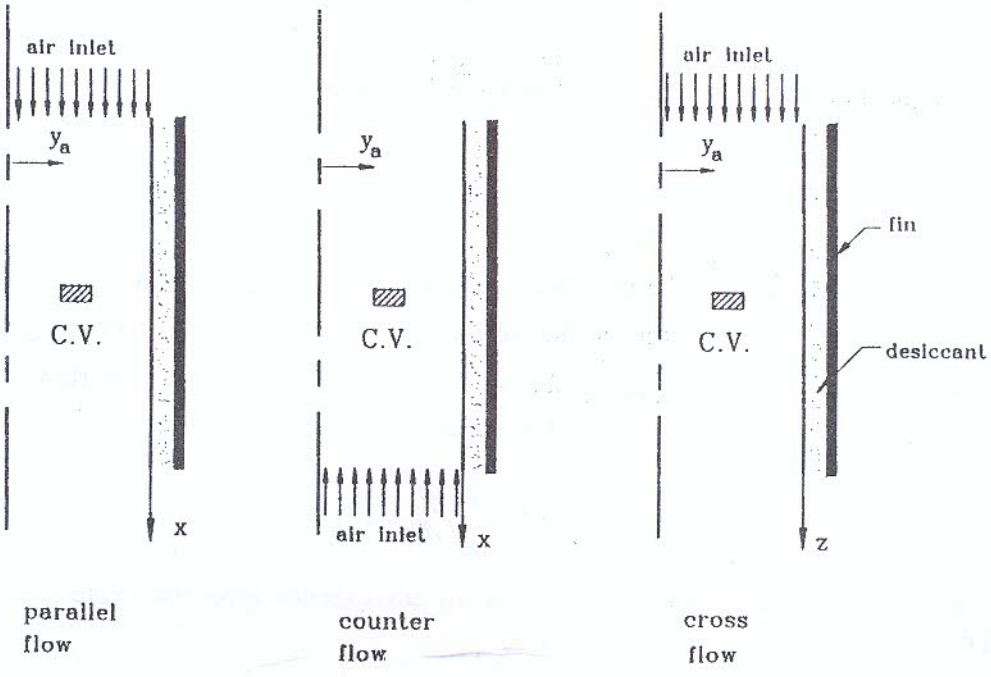

Fig. 4: The control volume of the air for the three flow configurations

Where, η is a coordinate in the air flow direction ($\eta = x$ for parallel flow, $\eta = -x$ for counter flow, and $\eta = z$ for cross flow). Equations 9 and 10 are subjected to the following boundary conditions at air entrance and at the center between the two fins

$$\text{at } \eta = 0: \qquad T_a = T_{ai}, \quad \omega = \omega_i \tag{10}$$

$$\text{at } y_a = 0: \qquad \frac{\partial T_a}{\partial y_a} = 0, \quad \frac{\partial \omega}{\partial y_a} = 0 \tag{11}$$

Equations 1, 2, 8, and 9 are subjected to the following continuity conditions at the air-liquid interface (i.e. at $y_d = \delta_d$ and $y_a = \delta_a$)

$$k_d \frac{\partial T_d}{\partial y_d} = -k_a \frac{\partial T_a}{\partial y_a} - \rho_a D_a \frac{\partial \omega}{\partial y_a} h_{fg} \tag{12}$$

$$\rho_d D_d \frac{\partial \zeta}{\partial y_d} = -\rho_a D_a \frac{\partial \omega}{\partial y_a} \tag{13}$$

$$\omega = \omega^*(T_d, \zeta)_{y_d = \delta_d}, \tag{14}$$

$$T_a = (T_d)_{y_d=\delta_d} \tag{15}$$

The momentum equation in the direction of the air flow is

$$\mu \frac{\partial^2 u_a}{\partial y_a^2} = \frac{dP}{d\eta} \tag{16}$$

The boundary conditions for the above equation are $\partial u_a / \partial y_a = 0$ at $y_a = 0$ and $u_a = a$ at $y_a = \delta_a$ (no slip at the air-liquid interface) where $a = (u_d)_{y_d=\delta_d}$ for parallel flow and $a = -(u_d)_{y_d=\delta_d}$ for counter flow and $a = 0$ for cross flow. The solution of the Eq. (16) with its boundary conditions gives

$$u_a = a - \frac{1}{2\mu}\frac{dP}{d\eta}(\delta_a^2 - y_a^2) \tag{17}$$

The continuity equation for the air flow at any cross section gives the expression for the pressure drop as

$$\frac{dP}{d\eta} = \frac{3\mu}{\delta_a^2}\left[a - \frac{\dot{m}_a}{2\rho_a \delta_a B}\right] \tag{18}$$

2.3 Fin Surface Temperature

To solve the energy and water concentration equations, the fin surface temperature distribution T_w is needed. Heat is transferred from the liquid desiccant to the fin surface then to the tube. The heat transfer coefficient between the liquid desiccant and the wall of the fin and the liquid desiccant temperature are not constants but they vary on the surface of the fin. These make the fin surface temperature varies on the fin surface in x and z directions. To find this distribution, the two-dimensional heat conduction equation is solved using finite difference technique. A finite difference mesh is considered to cover the surface of the fin. The conservation of energy for steady state heat transfer is applied for all the nodes of the mesh (the rate of heat transfer from the liquid film to the fin surface by convection is equal to the rate of heat transfer by conduction through x and z directions). For example, the energy equation for the node (i , k) is:

$$T_{w(i,k-1)} + T_{w(i-1,k)} + T_{w(i,k+1)} + T_{w(i+1,k)} - 4T_{w(i,k)} + 2\frac{h_d}{k\,t}(T_d - T_{w(i,k)}) = 0 \tag{19}$$

The local heat transfer coefficient between the liquid film and the surface of the fin is given by

$$h_d = \frac{k_d (\partial T_d / \partial y_d)_{y_d=0}}{(T_d - T_{w(i,k)})} \tag{20}$$

3. NUMERICAL SOLUTION

The governing equations were descritized using the control volume approach (see Patanker [8]). The coupling of the governing equations of the air and film flows with those of the temperature at the fin surfaces increases the complexity of the solution. An upwind technique was adopted for the convection terms of both flows of air and desiccant. This makes the descritized finite difference equations for air temperature and humidity ratio are dependent on the direction of air flow, i.e. the flow configuration. The solution of the finite difference equations was carried out by iteration method according to the algorithm given by Rahmah et al. [7] for parallel flow configuration.

4. ANALYSIS OF CALCULATED RESULTS

To assist in the analysis and presentation of the results, the following average quantities are defined. Let Γ stand for T_a, T_d, w, or ζ. The y-averaged value of Γ at given values of x and z is then defined as follows

$$(\overline{\Gamma})_y = \frac{1}{\overline{u}\delta} \int_0^{\delta} u\Gamma dy \tag{21}$$

where δ stands for δ_a or δ_d and u stands for the velocity of the flow under consideration. Similarly, the average value of Γ at any y-z plane for a given value of x is defined as

$$(\overline{\Gamma})_{yz} = \frac{1}{B} \int_0^{B} (\overline{\Gamma})_y dz \tag{22}$$

The average value of Γ for the entire flow is also defined by the following relation

$$(\overline{\Gamma})_{av} = \frac{1}{BH} \int_0^{H} \int_0^{B} (\overline{\Gamma})_y dz dx \tag{23}$$

The average wall temperature of the fin will be

$$\overline{T}_w = \frac{1}{BH} \int_0^{H} \int_0^{B} T_w dz dx \tag{24}$$

5. RESULTS AND DISCUSSION

Calculations were carried out to predict the variation of the temperature and water content of both the air and desiccant film along the fin surface. Calcium chloride ($CaCL_2$) solution was used as the liquid desiccant. Correlations were developed and used in the program to predict the properties of $CaCl_2$ solution in terms of T_d and ζ. Table 1 shows the values of the single cell design and supposed operating parameters that were used in the study for the two different processes: (1) air dehumidification process and (2) desiccant regeneration process. In the table, the symbol T_b refers to the base temperature of the fin, i.e. the temperature of the fin surface at contact with the tube. This temperature was used as a boundary condition to find the distribution of the fin surface temperature T_w.

Table 1 Design and supposed operating parameters of the single cell.

arameter		Air dehumidification		Desiccant regeneration	
		Basic value	range	Basic value	Range
T_{ai}	(°C)	35	25 - 40	40	35 - 45
$\omega_i \times 10^3$	(kg_w /kg_a)	20	15 - 25	20	15 - 25
T_{di}	(°C)	25	20 - 30	40	30 - 45
ζ_i	(kg_w /kg_s)	0.6	0.6 - 0.7	0.6	0.65 - 0.6
$m'_a \times 10^3$	(kg/m.s)	13.33	10 -16.6	13.33	10 -16.6
$m'_d \times 10^3$	(kg/m.s)	7	4 -10	7	4 -10
T_b	(°C)	10	10	60	60
f_s	(m)	0.0033	0.0033	0.0033	0.0033
H	(m)	0.03	0.03	0.03	0.03

A parametric study was carried out to predict the effect of changing $T_{ai}, \omega_i, T_{di}, \zeta_i, m_a$ and m_d on the heat and mass transfer process. It was found that, for the three flow configurations: (a) increasing the inlet temperature and the inlet water concentration of the liquid desiccant increase the air outlet temperature and the outlet humidity ratio. This can be attributed to the increase of the equilibrium humidity ratio of the air at the interface, (b) increasing the inlet air humidity ratio leads to more water vapor absorbed by the desiccant but this did not prevent the increase of the outlet humidity ratio of the air, and (c) decreasing the inlet water concentration of the liquid desiccant leads to more dehumidification of the air. This is due to the decrease in the equilibrium humidity ratio at the interface. These trends were consistent with those obtained for parallel flow by Rahmah et al. [7].

The effect of changing the mass flow rate of the air on the outlet conditions is shown in Fig. 5 for the three flow configurations. As shown in the figure increasing the air flow rate increases the outlet temperature and the outlet humidity ratio of the air, i.e. decreasing the cooling and dehumidification of the air. This can be attributed to the

increase of the velocity of the air which leads to the decrease of the time of contact between the air and the desiccant film. As shown in the figure parallel flow gives more cooling and dehumidification than the other configurations. This, also, can be attributed to the relative velocity between the air and the desiccant liquid film. The parallel flow has smaller relative velocity than the other configurations. The decrease of the relative velocity increases the time of contact which leads to more cooling and dehumidification.

The effect of changing the desiccant mass flow rate on the average outlet conditions of the air is shown in Fig. 6. As shown in the figure, increasing the liquid desiccant mass flow rate increases the outlet air temperature, i.e. decreasing the cooling capacity. This can be attributed to the increase of the thermal resistance of the liquid film as a result of increasing its thickness. Also the figure shows the increase of the outlet humidity ratio of the air with the increase of the liquid desiccant flow rate. This can be attributed to the increase of the temperature of the liquid desiccant film which leads to the increase of the equilibrium humidity ratio. Also the figure shows that the parallel flow configuration gives more cooling and dehumidification than the other two configurations. The distribution of the average desiccant temperature and the average air temperature along the surface of the fin are shown in Fig. 7 for the three flow configurations. As shown in the figure, the desiccant temperature increases as we move away from the center either in the x or z direction. This can be attributed to the temperature distribution of the surface of the fin which is minimum around the center and increases moving outward. Figure 7, also shows that the average air temperature is symmetric around z = 0.015 m for parallel and counter flow and the temperature decreases as the axial distance (measured from the inlet) increases. For cross flow the average temperature of the air decreases as z increases and the distribution is not symmetric around x = 0.015 m. This is due to the unsymmetrical liquid desiccant temperature distribution around x = 0.015 m.

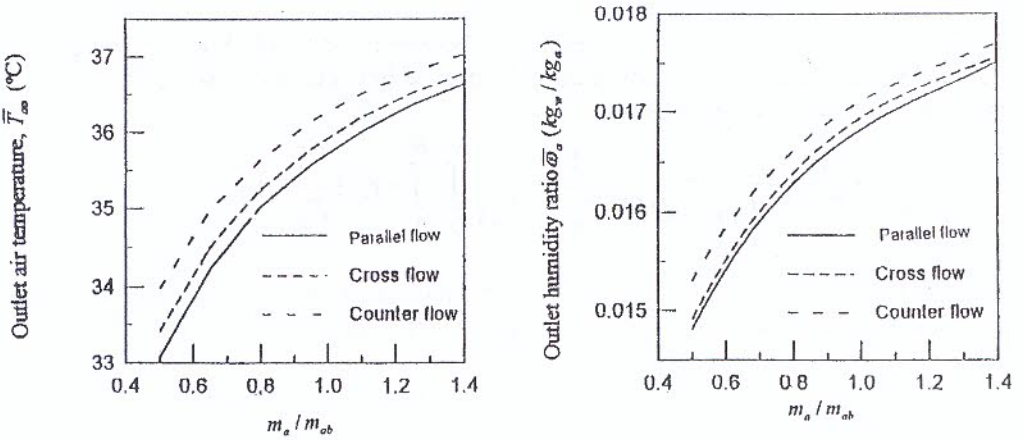

Fig. 5 Outlet air conditions for different air flow rates (air cooling+ dehumidification with T_{ai}=40 °C)

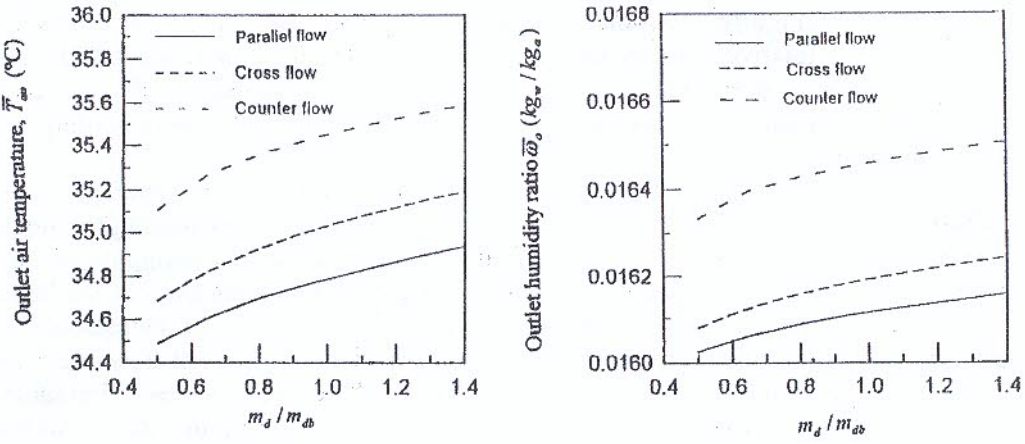

Fig. 6 Outlet air conditions for different desiccant flow rates (air cooling +dehumidification with T_{ai}=40 °C)

The effect of changing the air and liquid desiccant mass flow rates on the average outlet condition of the air during the regeneration process are shown in Figs. 8 & 9, respectively. As shown in the figures, increasing the air or liquid desiccant mass flow rates during the regeneration process lead to decreasing of the mass transfer from the desiccant to the air flow. This can be attributed to the same reasons discussed above.

6. HEAT AND MASS TRANSFER CORRELATIONS

The average heat transfer coefficient between the cooled air and the liquid desiccant film based on the temperature difference between the base of the fin and the inlet air can be defined as follows

$$\overline{h} = \frac{Q}{BH(T_{ai} - T_b)} = \frac{1}{BH(T_{ai} - T_b)} \int_0^H \int_0^B - k_a \left(\frac{\partial T_a}{\partial y_a}\right)_{y_a = \delta_a} dzdx \qquad (25)$$

where, Q is the heat transfer by convection from the air to the desiccant at the liquid-air interface surface. The average Nusselt number is then defined as

$$\overline{Nu} = \frac{4\delta_a \overline{h}}{k_a} = \frac{4\delta_a}{k_a BH(T_{ai} - T_b)} \int_0^H \int_0^B - k_a \left(\frac{\partial T_a}{\partial y_a}\right)_{y_a = \delta_a} dzdx \qquad (26)$$

where $4\delta_a$ is the hydraulic diameter of the single cell.

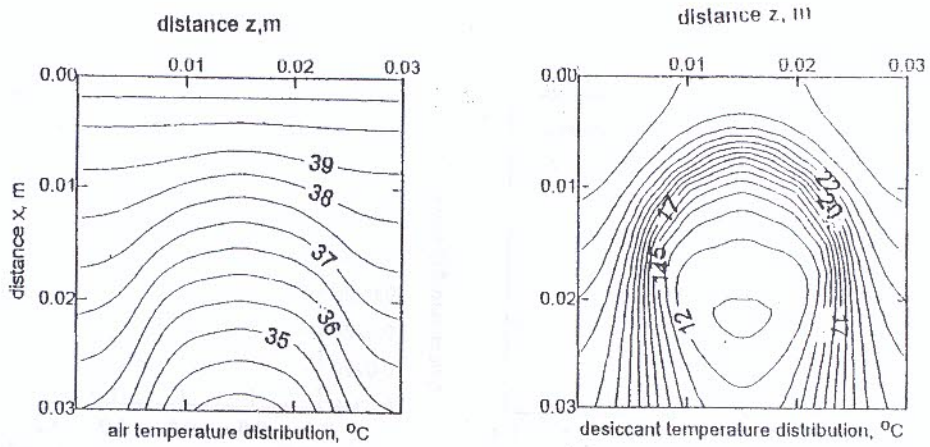

(a) parallel flow

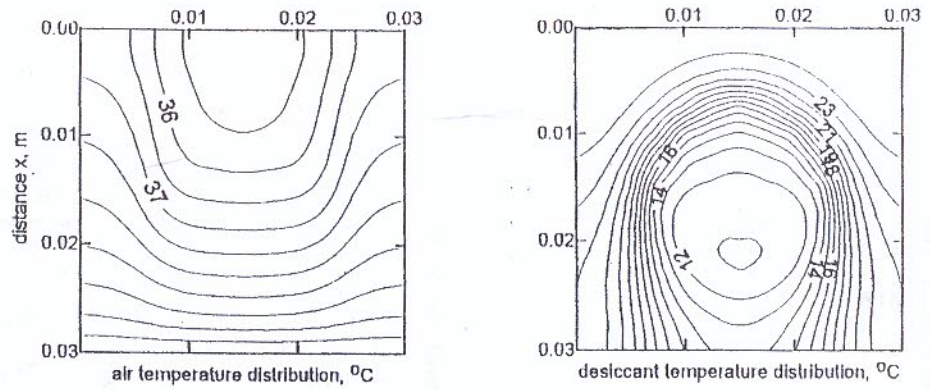

(b) counter flow

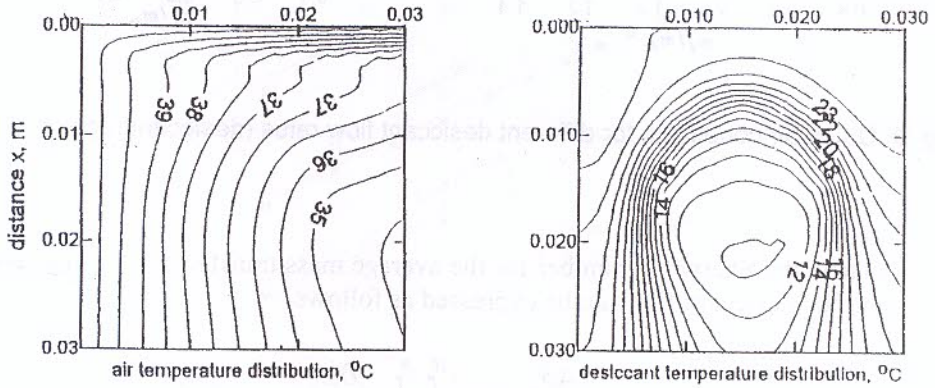

(c) cross flow

Fig. 7 Temperature contours (air cooling + dehumidification)

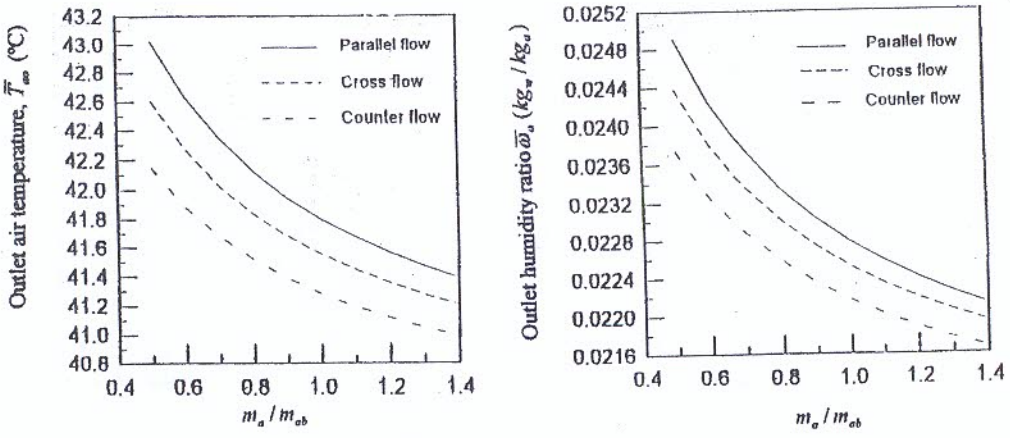

Fig. 8 Outlet air conditions for different air flow rates (desiccant regeneration).

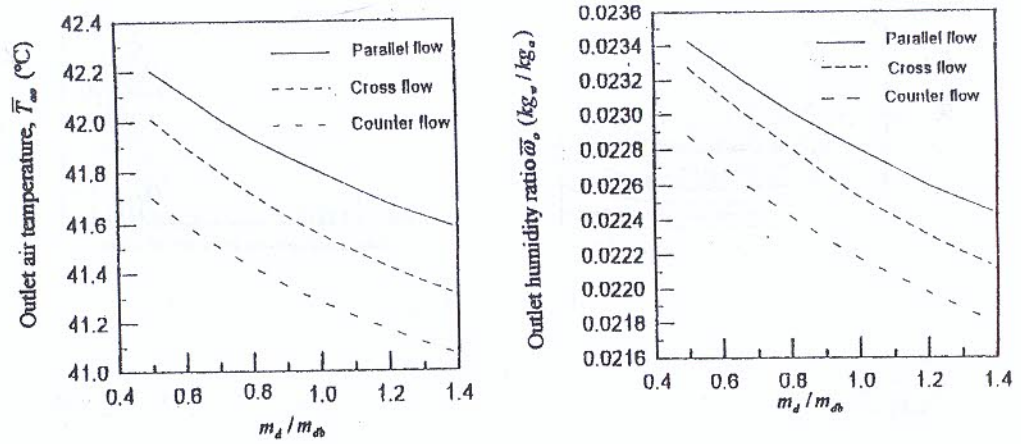

Fig. 9 Outlet air conditions for different desiccant flow rates (desiccant regeneration).

Similarly, the Sherwood number for the average mass transfer coefficient between the air and the desiccant film can be expressed as follows

$$\overline{Sh} = \frac{4\delta_a \overline{h}_{ma}}{\rho_a D_a} = \frac{4\delta_a}{BH(\omega_{ai} - \omega^*_b)} \int_0^H \int_0^B -\left(\frac{\partial \omega_a}{\partial y_a}\right)_{y_a=\delta_a} dzdx \qquad (27)$$

where ω_b^* is the equilibrium humidity ratio for air at temperature equals to the base temperature.

The variation of $\overline{Nu}$ and $\overline{Sh}$ with Reynolds number of the air flow ($\mathrm{Re} = 4\delta_a \overline{u}_a / \upsilon_a$) using the values for different operating conditions for air dehumidification given in Table 1 is shown in Fig. 10 for the three flow configurations. Considering the similarity between heat and mass transfer processes, the results were correlated for the three different air flow configurations by

$$\overline{Nu} / \mathrm{Pr}^a = b\ \mathrm{Re}^c$$
$$\overline{Sh} / Sc^a = b\ \mathrm{Re}^c \tag{28}$$

In the above correlations Pr and Sc are the Prandtl number and the Schmidt number for the air, respectively, and the constants a, b and c for the different flow configurations are shown in Table 2. To demonstrate the accuracy of the above correlations, these correlations are used to predict the average outlet humidity ratio and the average outlet air temperature $\overline{T}_{ao}$ from the following balances equations

$$m_a(\overline{\omega}_i - \omega_o) = \overline{h}_{ma} BH(\omega_i - \omega_b^*) \tag{29}$$

$$m_a C_{pa}(\overline{T}_{ai} - T_{ao}) = \overline{h}_a BH(T_{ai} - T_b) + m_a(\omega_i - \overline{\omega}_o) h_{fg} \tag{30}$$

These values of $\overline{T}_{ao}$ and $\overline{\omega}_o$ are compared with those directly obtained from the mathematical simulation computer program and the agreement was found fair enough.

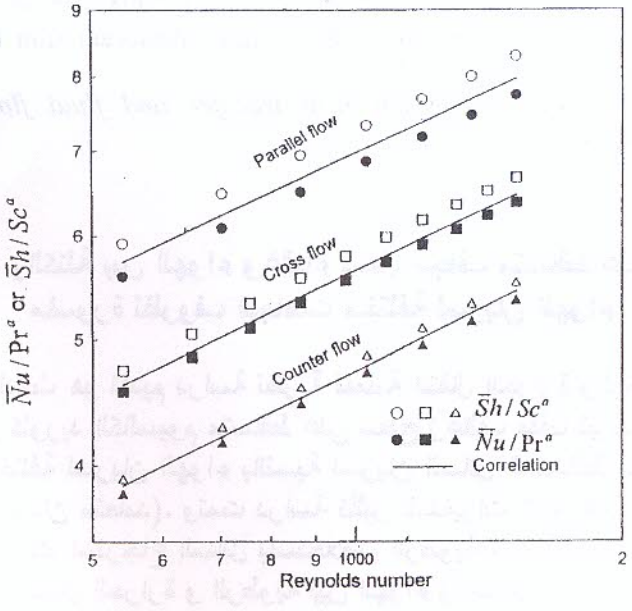

Fig.10 Variation of Nusselt and Sherwood numbers with Reynolds number.

8. CONCLUSIONS

A study was carried out to investigate the heat and mass transfer processes between parallel, counter and cross flow of air and a falling liquid desiccant film in a fin-tube arrangement. Correlations were developed to predict the average coefficient of heat and mass transfer in the air side. These correlations may be used to predict the average outlet air temperature and humidity ratio from the fin-tube geometry for the different flow configurations. Also the study concluded that the parallel flow of air relative to the falling desiccant film gives more cooling and dehumidification.

REFERENCES

1. Factor, H.M., G. Grossman. 1980. A packed bed dehumidifier/regenerator for solar air conditioning using liquid desiccant. *Solar Energy* 24:. 541-550.
2. Lof, G.O.G., T.G. Lenz and S. Rao. 1994. Coefficient of heat and mass transfer in a Packed bed suitable for solar regeneration of aqueous lithium chloride solution, *Trans. ASME, JSEE* 106: 387-392.
3. Saleh, F.E., M.G. Morsy, A.S. Huzayyin, and A.K. Abdel-Rahman. 1990. Experimental investigation of lithium chloride as a desiccant for air conditioning. *Bulletin of the faculty of engineering, Assiut university* 18(1): 52-59.
4. Elsayed, M.M. 1994. Analysis of air dehumidification using liquid desiccant system. *Renewable Energy*, 4(5): 519-528.
5. Khan, A.Y., and Ball, H.D. 1993. Experimental performance verification of a coil-type liquid desiccant system at part load operation. *Solar Energy* 51(5): 401-408.
6. Park, M.S., J.R. Howell, G.C. Vilet and J. Peterson. 1994. Numerical and experimental results for coupled heat and mass transfer between a Desiccant film and air in cross flow. *Int. J. Heat and Mass Transfer* 37 (Supple 1): 395-402.
7. Rahmah, A.S., M.M. Elsayed, and N.M. Al-Najem. 1998. A numerical solution of cooling and dehumidification of air by a falling desiccant film in parallel flow. *Renewable Energy* 13(3): 305-322.
8. Patanker, S.V. 1980. *Numerical heat transfer and fluid flow.* Hemisphere publishing corporation.

انتقال الحرارة والكتلة بين الهواء وغشاء سائل مجفف متساقط على سطح زعانف ماسورة لظروف اتجاهات مختلفة لسريان الهواء

الغرض من هذا البحث هو تقديم دراسة نظرية لعملية انتقال الحرارة والرطوبة بين الهواء وغشاء سائل من كلوريد الكالسيوم متساقط على سطح زعانف ملف تبريد. وتمت الدراسة لثلاث اتجاهات مختلفة لسريان الهواء بالنسبة لسريان السائل المتساقط (سريان متوازى- سريان عكسى- سريان متعامد). وتمت دراسة تأثير المتغيرات المختلفة على عملية تبريد وتجفيف الهواء وكذلك استرجاع السائل باستخلاص الرطوبة منه. وتم استنباط علاقات نظرية تعطى معدل انتقال الحرارة و الرطوبة بين الهواء و السائل الماص للرطوبة.

JES

مجلة العلوم الهندسية

المجلد ٣١ العدد ٢ أبريل ٢٠٠٣

الناشر كلية الهندسة-جامعة أسيوط-مصر